IEEJ Journal of Industry Applications
Vol.8 No.2 pp.279–286 DOI: 10.1541/ieejjia.8.279

Paper

A Control Strategy for Electro-hydrostatic Actuator Considering Static Friction, Resonance, and Oil Leakage

Sho Sakaino[*,**] Senior Member, Tomoki Sakuma[**] Non-member
Toshiaki Tsuji[**] Senior Member

(Manuscript received May 8, 2018, revised June 29, 2018)

Electro-hydrostatic actuators (EHAs) are hydraulic systems that operate without control valves, making them a compact, cheap, and highly energy efficient system. However, resonance, static friction, and oil leakage degrade their control performance. Three controllers are integrated to overcome these issues. First, static friction is suppressed by a feedback modulator (FM). Input torque is quantized to exceed the maximum static friction force, and quantization errors are suppressed by the FM. Second, resonance is canceled out by a self resonance cancellation (SRC) technique. In the SRC, both angle responses of a hydraulic pump and a hydraulic motor are measured, and the rigid body mode is extracted. Then, resonance becomes unobservable, changing the system as a second-order system. Third, modeling errors, including oil leakage, are suppressed by a self resonance cancellation disturbance observer (SRCDOB). As the SRCDOB is implemented in the rigid body mode, the cut-off frequency of the SRCDOB can be greater than that of most common disturbance observers. This combination of controllers drastically improves the control performance, and it enables control system design based on frequency.

Keywords: electro-hydrostatic actuator, hydraulic motor, two-mass resonant system, self resonance cancellation

1. Introduction

Hydraulic actuators are commonly utilized in robots requiring large amount of power, more than 500 W for each actuator, owing to their high power/weight ratios. Many studies have been performed on legged robots: BigDog [(1)], HyQ2Max [(2)], and TaeMu [(3)]. These actuators are driven by hydraulic pumps and the flow rate is controlled by servo valves. Rapid and powerful motion of legged robots has been achieved owing to the drastic improvement in the control frequency of servo valves. We also showed the effectiveness of hydraulic actuators for use in teleoperation robots [(4)(5)] enabling bilateral position and force transmission [(6)(7)]. Many effective methods to compensate for the inherent nonlinearities in servo valves have also been reported to improve the control performance of hydraulic actuators [(8)–(11)]. Therefore, the control theory for hydraulic actuators seems to be nearly complete.

However, servo valves have some drawbacks. First, servo valves are expensive. Second, the energy efficiency is low because hydraulic pumps are always in operation, even when the hydraulic actuators stop. Third, the entire system is large because most of the oil flow is regulated by servo valves and is returned to oil tanks, resulting in large tanks.

To overcome these inherent drawbacks, a different type of hydraulic system with closed oil circuits has been proposed.

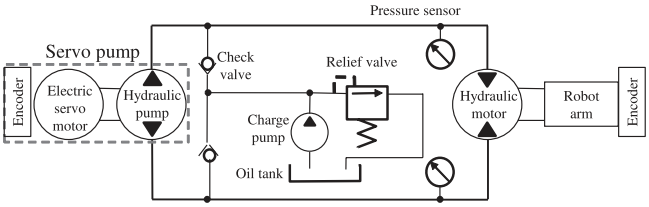

Fig. 1. Electro-hydrostatic actuator

This closed hydraulic circuit is called an electro-hydrostatic actuator (EHA) and is shown in Fig. 1. In EHAs, oil flow is controlled by servo pumps instead of servo valves. Servo pumps are composed of hydraulic pumps and servomotors that are coupled with the hydraulic pumps. Furthermore, EHAs are cost effective. In addition, servo pumps drive hydraulic actuators only when it is necessary, which drastically improves energy efficiency and reduces the size of tanks. It results in high energy efficiency especially in stopping. Needless to say, robots repeatedly move and stop in their operation. For that reason EHAs are suitable for robots driven by hydraulic actuators, and many studies regarding EHAs have been reported [(12)–(15)]. Since there is no nonlinear element due to servo valves, the control structure of EHAs is relatively simple. In addition, robots with EHAs have high backdrivability, making them useful for human assist robots [(16)(17)]. It is known empirically that the control performance of EHAs is not optimal. However the quantitative reasons for this have not been clear.

Recently, authors' research group revealed the reason for the poor control performance. Since static friction has large effects on the control performance of EHAs, a feedback

[*] JST, PRESTO
255, Shimo-okubo, Sakura-ku, Saitama 338-8570, Japan
[**] Graduate School of Science and Engineering, Saitama University
255, Shimo-okubo, Sakura-ku, Saitama, 338-8570 Japan

modulator (FM) [18], which is a static friction compensator, was implemented. In addition, oil leakage can be neglected at a high speed. Then, the dynamics of EHAs was identified using the motion data at a high speed. Since motor-sides (servo pumps) and load-sides (hydraulic actuators) can be regarded as independent inertias connected by elastic oil, EHAs can be modeled as two-mass resonant systems [19]. It is the resonance from elasticity that limits the control bandwidth. Although some of the conventional controllers are designed considering oil compression [12][13], they did not mention the resonance and controllers cannot be designed based on frequency characteristics.

Vibration suppression of two-mass resonant systems has been a popular research topic in the field of electric motors. Resonance ratio control is a practical way to design position controllers with resonance [20]–[22]. Full state feedback controllers have also been proposed to improve the performance [23]–[25]. In addition, self resonance cancellation (SRC), which is a method to cancel out the effect of resonance, has also been proposed [26][27]. In this method, rigid body modes of two-mass resonant systems are extracted, and the designers can tune the control parameters as if the systems are common second order systems.

Then, the authors exploit the conventional techniques associated with EHAs with the help of FMs, which are static friction compensators [28]. Resonance ratio control was implemented to obtain stable step responses [19]. The SRC was also implemented to achieve wide control bandwidth [29]. A state space, in which the effect of oil leakage can be neglected, was proposed to achieve full state feedback control of EHAs [30]. As a result, position control performance was improved even with elastic action caused by oil compression.

Oil leakage at a low speed is the last problem to be solved. In this paper, a self resonance cancellation disturbance observer (SRCDOB) [31] is implemented to estimate disturbances including the effect of oil leakage. Because the SRCDOB is implemented in rigid body modes, the cut-off frequency of the SRCDOB can be greater than that for other disturbance observers (DOBs). Therefore, in this study, three controllers are integrated to overcome the performance deterioration of EHAs. First, static friction is compensated by the FM. Second, the effect of resonance is canceled out by the SRC. Third, oil leakage is compensated by using the SRCDOB. Although each of these three methods have been conventionally proposed, this paper shows that the combination of these controllers can realize state-of-the-art control performance. Since no researcher except for authors regard EHAs as two-mass resonance systems, the combination of these controllers is proposed for the first time. In addition, the controller designing is easy because parameters can be determined by frequency characteristics. The validity of the proposed method is experimentally verified.

The rest of the paper comprises the following sections. The model for EHAs is shown in section 2. Then, the proposed controller is explained in section 3. The validity of the proposed method is verified in section 4, and this paper is concluded in section 5.

2. Modeling

Figure 2 shows an overview of a robot used in this research.

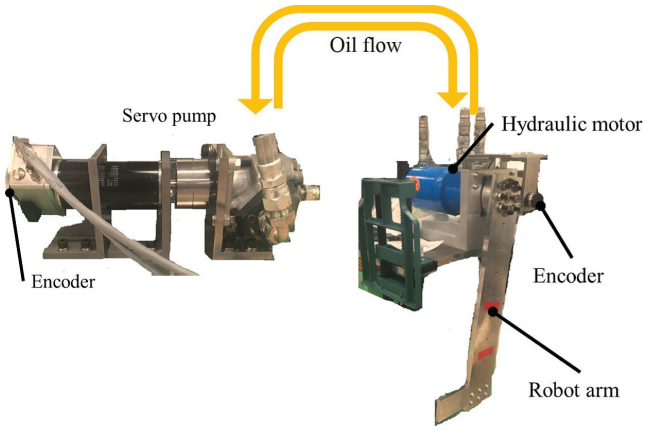

Fig. 2. Experimental setup

The robot has single degree of freedom. A servo pump, which directly controls oil flow, is composed of a servomotor (DC brushless motor E-60 made by MAXON) and a hydraulic gear pump (MA-03 made by EATON). The angle responses of the servomotor were measured by an absolute encoder with 17-bit resolution. A robot arm was attached to a hydraulic motor (S-380 made by EATON), and the hydraulic motor was driven by the oil flow from the servo pump. The angle responses of the robot arm were also measured by an absolute encoder with 17-bit resolution.

The dynamics of the motor-side is given as follows:

$$J_m(\ddot{\theta}_m^{res} - \ddot{\theta}_m^{leak}) + B_m(\dot{\theta}_m^{res} - \dot{\theta}_m^{leak}) = \tau_m^{ref} - \frac{D_m}{2\pi}p^{res} - \tau_m^{dis}. \quad \cdots\cdots (1)$$

where, J, B, D, τ, θ, and p represent the inertia, viscous coefficient, displacement, torque, angle, and pressure difference between input and output ports, respectively. Variables with the subscript m stand for motor-side values. The superscripts res, ref, and $leak$ stand for response values, reference values and the effect of oil leakage, respectively. Variables with the superscript dis are disturbance values, which include nonlinearities, static friction, and modeling errors. Many conventional methods explicitly model the nonlinear effects in EHAs resulting in difficulty for the controller designing. However, they can be precisely estimated by the SRCDOB as it is explained in the following section. Then, equation (1) can be simplified by regarding the effects of oil leakage as disturbances.

$$J_m\ddot{\theta}_m^{res} + B_m\dot{\theta}_m^{res} = \tau_m^{ref} - \frac{D_m}{2\pi}p^{res} - \tau_m^{dis'} \quad \cdots\cdots (2)$$
$$\tau_m^{dis'} = \tau_m^{dis} - J_m\ddot{\theta}_m^{leak} - B_m\dot{\theta}_m^{leak}$$

The dynamics of the load-side is given as follows:

$$J_l(\ddot{\theta}_l^{res} - \ddot{\theta}_l^{leak}) + B_l(\dot{\theta}_l^{res} - \dot{\theta}_l^{leak}) = \frac{D_l}{2\pi}p^{res} - \tau_l^{dis}. \quad \cdots\cdots (3)$$

Here, variables with the subscript l stand for load-side values. Then, this equation can also be simplified.

$$J_l\ddot{\theta}_l^{res} + B_l\dot{\theta}_l^{res} = \frac{D_l}{2\pi}p^{res} - \tau_l^{dis'} \quad \cdots\cdots (4)$$
$$\tau_l^{dis'} = \tau_l^{dis} - J_l\ddot{\theta}_l^{leak} - B_l\dot{\theta}_l^{leak}$$

The flow rate of the motor-side q_m and the load-side q_l are

given as follows:

$$q_m = \frac{D_m}{2\pi}(\dot{\theta}_m^{res} - \dot{\theta}_m^{leak}) \cdots\cdots (5)$$

$$q_l = \frac{D_l}{2\pi}(\dot{\theta}_l^{res} - \dot{\theta}_l^{leak}). \cdots\cdots (6)$$

Then, the pressure difference is generated by oil compression as follows:

$$p^{res} = \frac{1}{C_b s}(q_m - q_l) \cdots\cdots (7)$$

$$= \frac{1}{C_b s}\frac{D_m}{2\pi}(\dot{\theta}_m^{res} - \frac{D_l}{D_m}\dot{\theta}_l^{res} - \dot{\theta}^{leak}) \cdots\cdots (8)$$

$$\dot{\theta}^{leak} = \dot{\theta}_m^{leak} - \frac{D_l}{D_m}\dot{\theta}_l^{leak}$$

where, C_b is a compression coefficient.

By combining above equations, a block diagram of the EHA is derived as shown in Fig. 3. As the block diagram clearly shows, EHAs can be modeled as two-mass resonant systems. To identify the parameters, the FM [28] was implemented to eliminate the effect of static friction and the effect of oil leakage was eliminated by operating in a high-speed range where $\dot{\theta}_m^{leak}$ and $\dot{\theta}_l^{leak}$ can be ignored. Usually, oil leakage has speed dependent nonlinearities and it is considered in the controller designing. However, it results in too conservative controllers. The authors find that the phase delay is the main reason for performance degradation, and the parameters should better to be identified in the speed domain in which oil leakage can be neglected. However, the neglected oil leakage still deteriorates the performance in the conventional method [29]. Therefore, oil leakage is estimated as a disturbance using SRCDOB explained in 3.3 without knowing its explicit model.

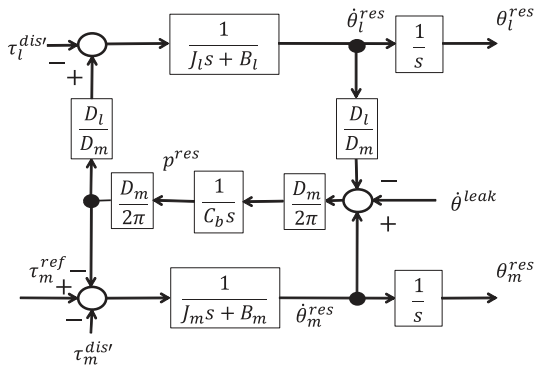

Fig. 3. Plant model of entire EHA

Table 1. Plant parameters

Inertia of motor-side J_m	kgm^2	0.00063
Inertia of load-side J_l	kgm^2	0.84
Viscous friction of motor-side B_m	Nms	0.0003
Viscous friction of load-side B_l	Nms	5.0
Displacement of motor-side D_m	cm^3/rev	3.08
Displacement of load-side D_l	cm^3/rev	390
Resonance frequency ω_p	rad/s	43.68
Anti-resonance frequency ω_z	rad/s	42.08

Figure 4 shows the frequency characteristics of the EHA: $\frac{\theta_m^{res}}{\tau_m^{ref}}$ and $\frac{\theta_l^{res}}{\tau_m^{ref}}$. Blue and green lines indicate a motor-side response and its model. Red and orange lines indicate a load-side response and its model. The left and right figures show the gain and phase. Although the gain around the resonance frequency does not match because of the nonlinearity, the phase precisely explains the dynamics of the EHA. The identified parameters are shown in Table 1.

3. Controller

In the conventional method, two of the three problems associated with EHAs, i.e., static friction and resonance, were solved using the FM and SRC. We proposed the implementation of the SRCDOB to eliminate the rest of the problem: the effect of oil leakage.

The controllers were implemented using C language with the Ubuntu Linux 14.04 on a personal computer with Intel Core i7 6700.

3.1 Feedback Modulator In the FM, a continuous input torque τ_C^{ref} is quantized to exceed the maximum static friction torque making the system free from static friction.

Theoretically, the quantized input torque τ_Q^{ref} can be an arbitrary value greater than the maximum static friction. However, if the input torque is greater than the maximum static friction, quantization is not needed and deteriorates power efficiency. Then, to suppress the power consumption, τ_Q^{ref} was set as follows:

$$\tau_Q^{ref} = \begin{cases} 0 & (\tau_C^{ref} = 0) \\ \tau_d \cdot \mathrm{sgn}(\tau_C^{ref}) & (0 < |\tau_C^{ref}| < \tau_d) \\ 2\tau_d \cdot \mathrm{sgn}(\tau_C^{ref}) & (\tau_d < |\tau_C^{ref}| < 2\tau_d) \\ \tau_C^{ref} & (2\tau_d < |\tau_C^{ref}|) \end{cases} \cdots\cdots (9)$$

where sgn$(\cdot)$ is a sign function and τ_d is a quantization value greater than the maximum static friction.

It is clear that the quantization generates quantization errors. The FM estimates and compensates for the errors as shown in Fig. 6. Here, $Q(s)$, which confirms $1 - Q(s) = (Ts/(Ts+1))^2$, is a low-pass filter. In addition, s is a Laplace

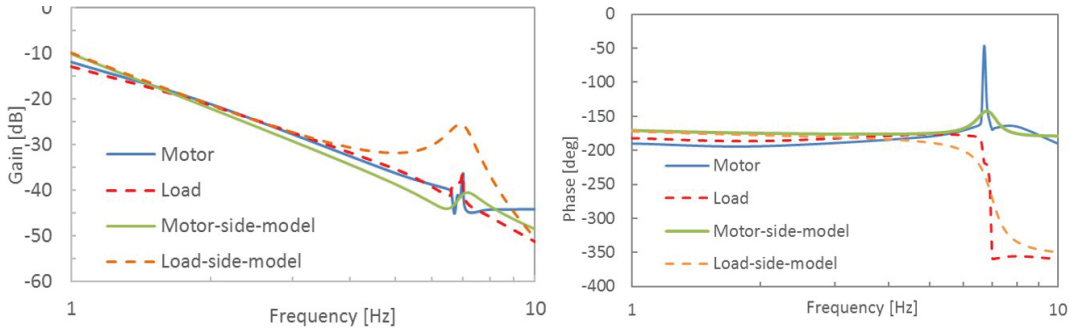

Fig. 4. Frequency characteristic of EHA

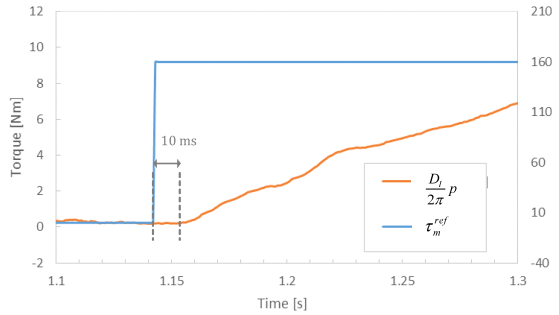

Fig. 5. Dead time

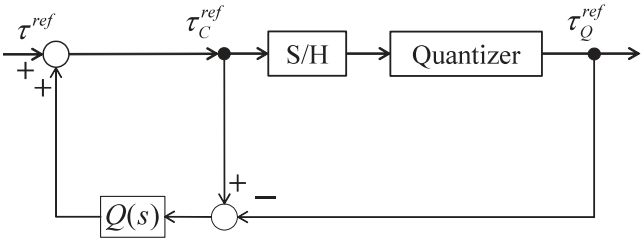

Fig. 6. Feedback modulator

operator. The time constant of the low-pass filter T was chosen such that it was sufficiently longer than the dead time between the torque reference and pressure. Figure 5 shows the dead time between an input torque on the motor-side and the input torque on the load-side, $\frac{D_l}{2\pi}p$. The dead time was found to be approximately 10 ms, so T was selected to be 21 ms. Note that the dead time is duration until the compression force exceeds the maximum static friction of the load-side. In addition, the FM is implemented by using z-transform as described in [32].

The quantization error $e = \tau_C^{ref} - \tau_Q^{ref}$ affects the original control input τ^{ref} as follows:

$$\tau_Q^{ref} = \tau^{ref} + (1 - Q(s))e. \cdots (10)$$

As Fig. 6 shows, the FM has a structure similar to a DOB [33] when we regard "quantization" as a real plant and "1" as a nominal inverse model of the plant. Hence, the quantization errors are treated as disturbances of the control input. In addition, there is no observation error of τ_Q^{ref} because the quantization errors are intentionally created. As a result, the time constant of the low-pass filter can be set to be far greater than the resonance frequency of the system, so the quantization errors will have very few effects on the control performance.

Then, the quantized control input is finally given to the motor-side.

$$\tau_m^{ref} = \tau_Q^{ref} \cdots (11)$$

3.2 Self Resonance Cancellation Next, the SRC is introduced. In the SRC, the effect of torsional vibration becomes unobservable by changing the system dynamics as a rigid body model [27]. In other words, the center of gravity of the motor- and load-side is controlled. Aoki *et al.* improved the conventional SRC by considering the effect of viscosity [31].

By canceling out p^{res} from equations (2) and (4), the following equation is obtained.

$$J_m\ddot{\theta}_m^{res} + B_m\dot{\theta}_m^{res} + \frac{D_m}{D_l}(J_l\ddot{\theta}_l^{res} + B_l\dot{\theta}_l^{res}) = \tau_m^{ref} - \tau_m^{dis'} - \frac{D_m}{D_l}\tau_l^{dis'} \cdots (12)$$

If we define an auxiliary value θ_{SRC} as (13) with a reduction ratio $R = \frac{D_l}{D_m}$, equation (12) in the Laplace domain is simplified in (14).

$$\theta_{SRC} = \left(J_m + \frac{B_m}{s}\right)\theta_m^{res} + \left(\frac{J_l}{R} + \frac{B_l}{sR}\right)\theta_l^{res} \cdots (13)$$

$$s^2\theta_{SRC} = \tau_m^{ref} - \tau_m^{dis'} - \frac{1}{R}\tau_l^{dis'} \cdots (14)$$

The control target is to regulate the following value, e_{SRC}, to be zero.

$$e_{SRC} = \left(J_m + \frac{B_m}{s}\right)(\theta_l^{cmd} - R\theta_m^{res}) + \left(\frac{J_l}{R} + \frac{B_l}{sR}\right)(\theta_l^{cmd} - \theta_l^{res}) \cdots (15)$$

Here, variables with the superscript *cmd* are command values. Because (14) is a simple second order system, a proportional derivative (PD) controller was implemented with proportional and derivative gains: $C_{FB} = K_p + K_v s$.

$$\tau_{SRC}^{ref} = C_{FB}e_{SRC} \cdots (16)$$

3.3 Self Resonance Cancellation Disturbance Observer As equation (14) shows the disturbance terms, especially those caused by oil leakage, deteriorate the control performance of the SRC. Then, a DOB is implemented in the dynamics (14) to estimate and suppress the disturbances.

The disturbances in (14) are estimated using a low-pass filter, Q_g.

$$\hat{\tau}_m^{dis'} + \frac{1}{R}\hat{\tau}_l^{dis'} = Q_g(\tau^{ref} - s^2\theta_{SRC}) \cdots (17)$$

$$Q_g = \frac{g}{s+g}$$

where, $\hat{\tau}_m^{dis'} + \frac{1}{R}\hat{\tau}_l^{dis'}$ is the estimate of the disturbances. Note that the control input without quantization, τ^{ref}, is used to estimate the disturbances instead of the actual control input, τ_m^{ref}, because the actual control input has high-frequency components caused by the FM.

Then, the disturbances are suppressed using the estimate of the disturbances.

$$\tau^{ref} = \tau_{SRC}^{ref} + Q_g(\tau^{ref} - s^2\theta_{SRC}) \cdots (18)$$

Because (14) is a rigid body mode, the cut-off frequency of the low-pass filter, g, can be far greater than that of the DOB on the motor-side. Since it is possible to estimate the disturbances by the high-gain-observer, detailed modeling of the disturbances becomes unnecessary, and control system design becomes very easy.

3.4 Overall Controller The whole controller is illustrated in Fig. 7. In this figure, parameters with the subscript n stand for nominal values. As equation (15) shows, the proposed controller does not make the load-side response follow the target value but instead regulates e_{SRC} to be zero. Therefore, at the first glance, it seems that the proposed method

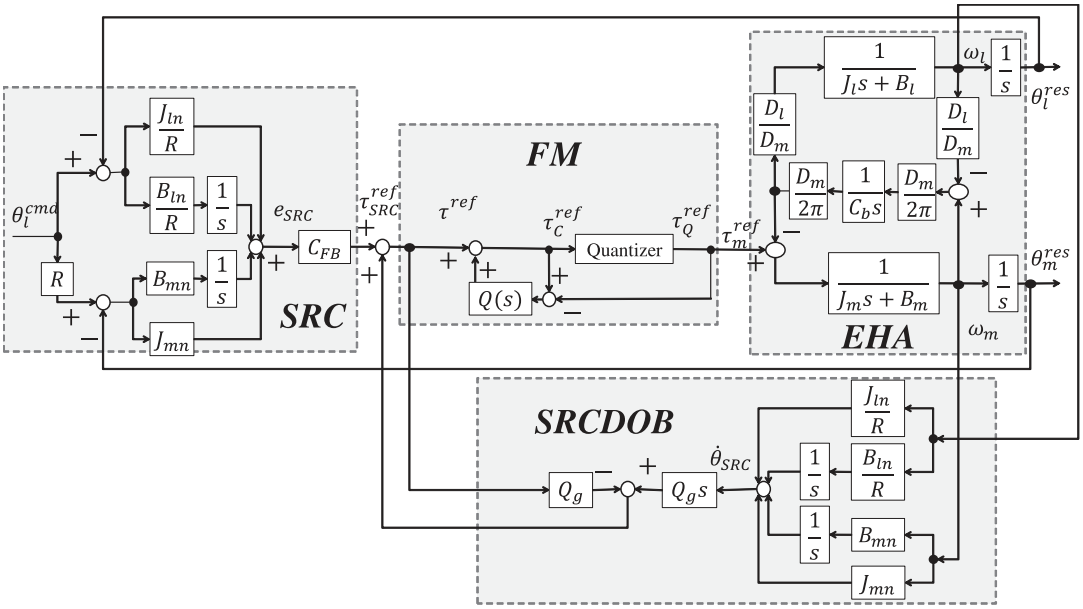

Fig. 7. Block diagram of whole controller

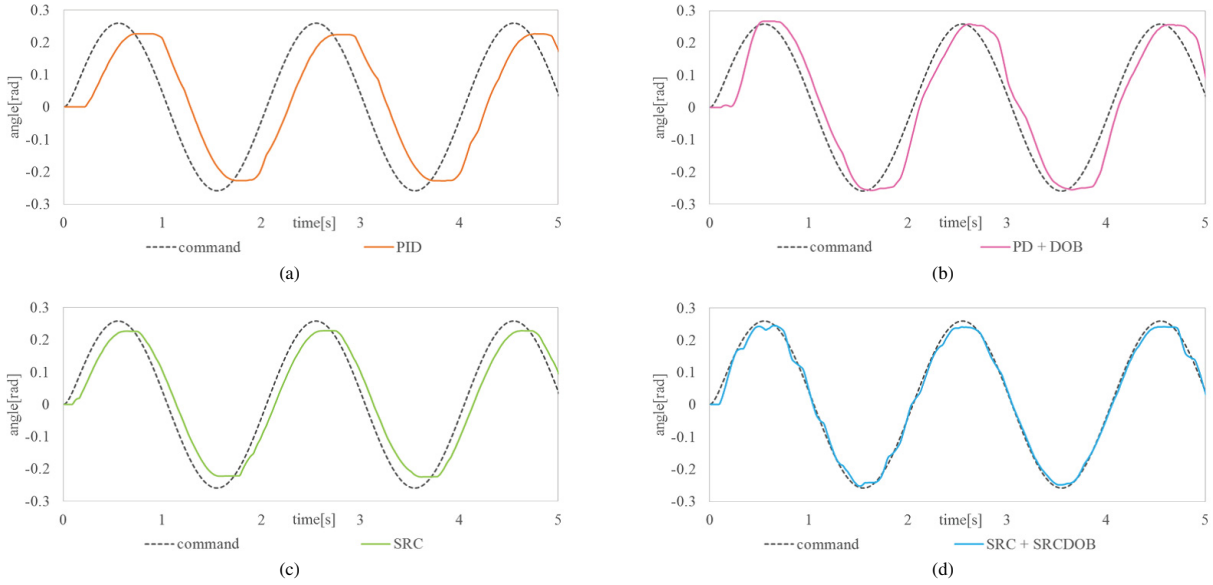

Fig. 8. Experimental results with 0.5 Hz sine wave: (a) PID controller, (b) PD controller + DOB, (c) SRC, (d) SRC + SRCDOB

does not satisfy the control requirements.

However, as shown in Table 1, the viscous friction of the motor-side is almost zero, so we set $B_{mn} = 0$. Therefore, only the load-side has an integrator in (15). As a result, the load-side response gradually tracks the command value [31] and the control requirements are satisfied.

4. Experiment

In this study, the proposed method was compared with the following three controllers: a proportional integral derivative (PID) controller, a PD controller with a DOB on the load-side [32], and the SRC [29]. The PID controller was implemented as follows:

$$\tau^{ref} = \left(\frac{K_i}{s} + K_p + K_v s\right)(\theta_l^{cmd} - \theta_l^{res}). \cdots\cdots\cdots\cdots (19)$$

In addition, the PD controller with the load-side disturbance observer was implemented as follows:

$$\tau_{PD}^{ref} = (K_p + K_v s)(\theta_l^{cmd} - \theta_l^{res}) \cdots\cdots\cdots\cdots\cdots\cdots (20)$$

$$\tau^{ref} = \tau_{PD}^{ref} + Q_g(\tau^{ref} - s^2 J_l \theta_l). \cdots\cdots\cdots\cdots\cdots\cdots (21)$$

The FM was implemented in every controller to suppress the effect of static friction. Each controller was designed so that the phase margin was 62 degrees. Then, the designed control bandwidth of the PID controller, the PD controller, and the SRC were 1.67 Hz, 1.72 Hz, and 2.69 Hz, respectively. This result clearly indicates that the control bandwidth can be broadened by considering the effect of resonance caused by oil compression. Velocities were obtained using pseudo differentiation of the angle responses. The control parameters are listed in Table 2. Note that because the DOB of the conventional method [32] was implemented on the load-side, the cut-off frequency could not be very high owing to oil compression. Conversely, the SRCDOB is free from oil compression because it is designed for a rigid body model,

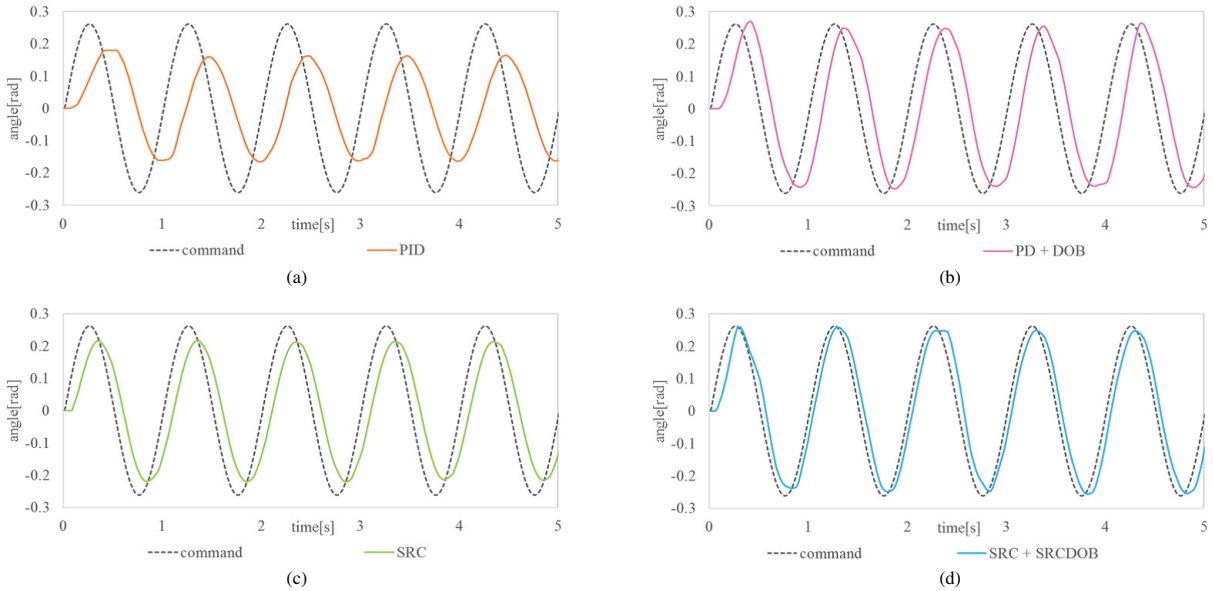

Fig. 9. Experimental results with 1.0 Hz sine wave: (a) PID controller, (b) PD controller + DOB, (c) SRC, (d) SRC + SRCDOB

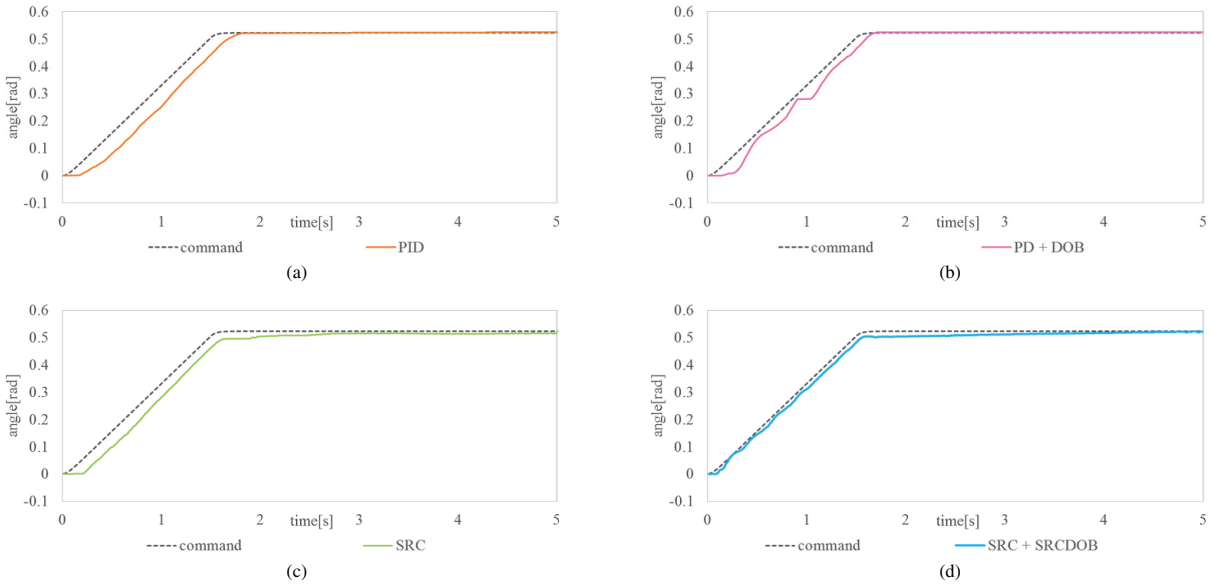

Fig. 10. Experimental results with ramp-shaped command: (a) PID controller, (b) PD controller + DOB, (c) SRC, (d) SRC + SRCDOB

Table 2. Control parameters

Sampling time T_s	s	0.001
Cut-off frequency of pseudo differential	rad/s	40.0
Proportional gain of SRC K_p		6100
Derivative gain of SRC K_v		1100
Proportional gain of PD K_p		380.25
Derivative gain of PD K_v		39
Proportional gain of PID K_i		361
Integral gain of PID K_p		105
Derivative gain of PID K_v		38
Cut-off frequency of DOB	rad/s	20.0
Cut-off frequency of SRCDOB g	rad/s	32.0
Quantization value τ_d	Nm	40.0

resulting in a higher cut-off frequency.

In this experiment, three commands were given to the four controllers: sine waves with frequencies of 0.5 and 1.0 Hz and a ramp-shaped trajectory. Figures 8–10 show the results. Dotted and solid lines show command values and response values, respectively. The PID controller, which is widely used for control of EHAs, showed quite poor control performance, as shown in Figs. 8(a) and 9(a). Both the magnitude and phase were far from ideal responses. As shown in Figs. 8(b) and 9(b), the magnitude of the responses was improved because oil leakage was compensated for by the DOB while the phase lag only slightly recovered. Conversely, Figs. 8(c) and 9(c) show that the phase lag was drastically improved with the use of the SRC although the magnitude was unsatisfactory because of the disturbances. Ultimately, the proposed method showed far better control performance both in terms of the magnitude and phase. It turns out that using both the SRC and the SRCDOB is important for obtaining a good response. In addition, the disturbance suppression characteristics were improved because the cut-off frequency of SRCDOB was higher than that of the DOB, and it also contributed to the improvement of the performance. Table 3 quantitatively evaluates the control performance using the

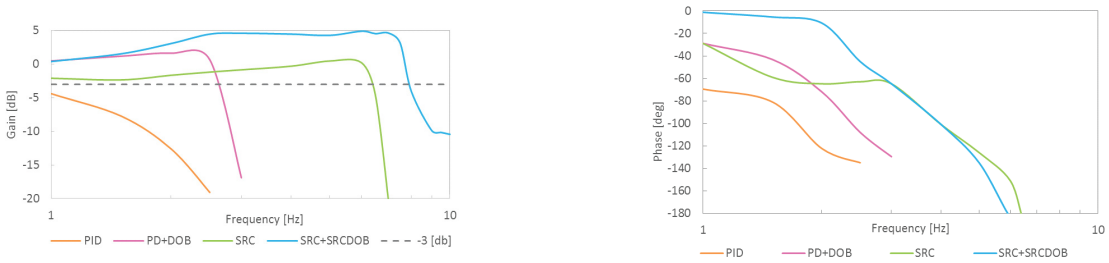

(a) (b)

Fig. 11. Closed loop bode plot of ($\frac{\theta_l^{res}}{\theta_l^{cmd}}$): (a)gain, (b)phase

Table 3. Root mean square error [rad]

	0.5 Hz	1.0 Hz
PID Controller	0.12	0.19
PD Controller + DOB	0.059	0.14
SRC	0.068	0.15
SRC + SRCDOB	0.011	0.10

root mean square error (RMSE). It also confirms the usefulness of the proposed method. Figure 10 shows that the proposed method drastically improved the transient response while the other three controllers showed large lags. However, the proposed method did not converge to the steady state as quickly. As discussed in 3.4, because the proposed method does not directly control the load-side, it entered a steady state slowly because of a weak integrator given by the load-side viscosity B_l. However, considering the drastic improvement in the sinusoidal responses and transient responses, this can be considered a trivial problem.

The closed loop bode plot of $\frac{\theta_l^{res}}{\theta_l^{cmd}}$ is described in Fig. 11. The control bandwidth of the proposed method was the widest; at the same time, the phase lag was the smallest. It should also be noted that the frequency at which the gain was -3 dB was higher than the resonance frequency of 7 Hz (43.68 rad/s).

The proposed method also has good robustness against modeling errors because the SRCDOB can treat the modeling errors as disturbances and suppress their effects. Figure 12 shows responses without modeling errors, with a modeling error on the motor-side $J_m = 2J_{mn}$, and with a modeling error on the load-side $J_l = 2J_{ln}$. There was almost no difference, even with the parameter perturbation because of the SRCDOB.

To the best of the authors' knowledge, there is no research treating the resonance of EHAs, except for that of the authors. As a result, it enables control system design based on frequency, and the state-of-the-art control performance was obtained.

5. Conclusion

Although the low control performance of EHA has been well known, a mathematical model has not been proposed. Recently, the authors revealed that this is due to resonance caused by oil compression. Although the authors proposed several methods for suppressing resonance [19][29][32], they do not demonstrate sufficient performance because oil leakage is not compensated for. Therefore, the authors proposed the implementation of the SRCDOB to compensate for oil leakage. Because it is implemented in a rigid body mode, a very high cut-off frequency can be set for the SRCDOB resulting

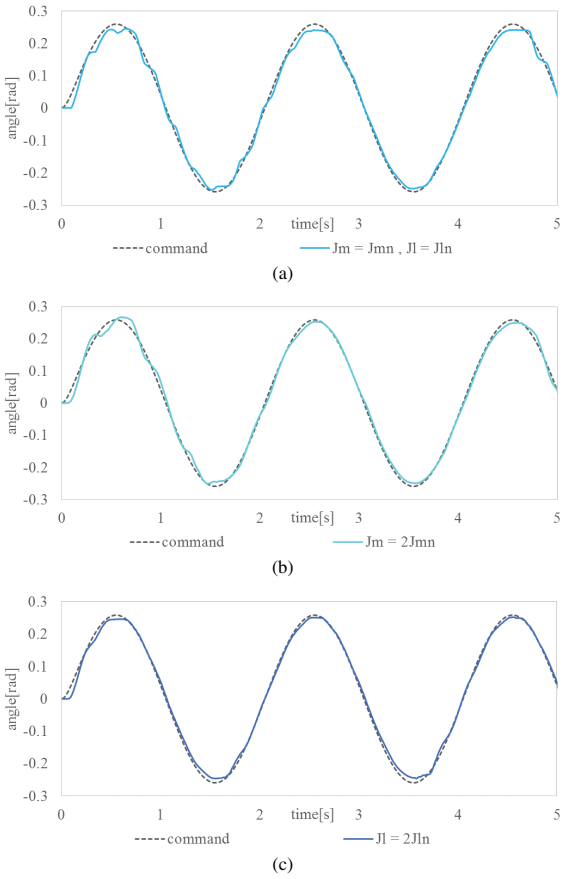

Fig. 12. Experimental result with modeling error: (a) $J_m = J_{mn}, J_l = J_{ln}$, (b) $J_m = 2J_{mn}$, (c) $J_l = 2J_{ln}$

in a highly robust system against modeling errors, including oil leakage. Experimental results demonstrated that the proposed method can improve oil leakage and phase lag, at the same time it showed high robustness. Our next goal is resonance suppression in EHAs with multiple degrees of freedom. At the same time, force control using EHAs is also our research target [34].

Acknowledgment

This research was supported by JSPS KAKENHI Grant Number 16K06410 and JST, PRESTO Grant Number JPMJPR1755, Japan.

References

(1) M. Raibert, K. Blankespoor, G. Nelson, R. Playter, and the BigDog Team: "Bigdog, the rough-terrain quadruped robot", in Proceedings of the 17th World Congress The International Federation of Automatic Control, pp.10822–10825 (2008)

(2) C. Semini, V. Barasuol, J. Goldsmith, M. Frigerio, M. Focchi, Y. Gao, and D.G. Caldwell: "Design of the hydraulically actuated, torque-controlled quadruped robot hyq2max", *IEEE/ASME Transactions on Mechatronics*, Vol.22, No.2, pp.635–646 (2017)

(3) S.-H. Hyon, D. Suewaka, Y. Torii, and N. Oku: "Design and experimental evaluation of a fast torque-controlled hydraulic humanoid robot", *IEEE/ASME Transactions on Mechatronics*, Vol.22, No.2, pp.623–634 (2017)

(4) S. Sakaino, T. Furuya, and T. Tsuji: "Bilateral control between electric and hydraulic actuators using linearization of hydraulic actuators", *IEEE Transactions on Industrial Electronics* (2017)

(5) K. Tsuda, S. Sakaino, and T. Tsuji: "Bilateral control between electric and electro-hydrostatic actuators using feedback modulator", in Proceedings of 42nd Annual Conference of the IEEE Industrial Electronics Society, pp.506–511 (2016)

(6) S. Sakaino, T. Sato, and K. Ohnishi: "A novel motion equation for general task description and analysis of mobile-hapto", *IEEE Transactions on Industrial Electronics*, Vol.60, No.7, pp.2673–2680 (2013)

(7) S. Sakaino, T. Sato, and K. Ohnishi: "Multi-dof micro macro bilateral controller using oblique coordinate control", *IEEE Transacsions on Industrial Informatics*, Vol.7, pp.446–454 (2011)

(8) C. Hu, B. Yao, and Q. Wang: "Performance-oriented adaptive robust control of a class of nonlinear systems preceded by unknown dead zone with comparative experimental results", *IEEE/ASME Transactions on Mechatronics*, Vol.18, pp.178–189 (2013)

(9) J. Yao, W. Deng, and Z. Jiao: "Adaptive control of hydraulic actuators with lugre model based friction compensation", *IEEE Transactions on Industrial Electronics*, Vol.62, pp.6469–6477 (2015)

(10) S. Dasmahapatra, B.K. Sarkar, R. Saha, A. Chatterjee, S. Mookherjee, and D. Sanyal: "Design of an adaptive fuzzy-bias smc and validation for a rugged electrohydraulic system", *IEEE/ASME Transactions on Mechatronics*, Vol.20, No.6, pp.2708–2715 (2015)

(11) T.H. Ho and K.K. Ahn: "Speed control of a hydraulic pressure coupling drive using an adaptive fuzzy sliding-mode control", *IEEE/ASME Transactions on Mechatronics*, Vol.17, pp.976–986 (2012)

(12) Y. Lin, Y. Shi, and R. Burton: "Modeling and robust discrete-time sliding-mode control design for a fluid power electrohydraulic actuator (eha) system", *IEEE/ASME Transactions on Mechatronics*, Vol.18, No.1, pp.1–10 (2013)

(13) W.Y. Lee, M.J. Kim, and W.K. Chung: "An approach to development of electro hydrostatic actuator (eha)-based robot joints", in Proceedings of 2015 IEEE International Conference on Industrial Technology, pp.99–106 (2015)

(14) J. won Lee, H. Kim, J. Jang, and S. Park: "An experimental study of the characteristics of hydrostatic transmission systems", *Journal of Advanced Robotics*, Vol.29, No.14, pp.939–946 (2015)

(15) S. Kukkonen and E. Makinen: "Performance of a pump controlled asymmetric actuator: A comparison of different control methods", in ASME/BATH 2014 Symposium on Fluid Power and Motion Control, pp.1–10 (2014)

(16) H. Kaminaga, H. Tanaka, and Y. Nakamura: "Mechanism and control of knee power augmenting device with backdrivable electro-hydrostatic actuator", in Proceedings of 13th World Congress in Mechanism and Machine Science (2011)

(17) H. Kaminaga, K. Odanaka, Y. Ando, S. Otsuki, and Y. Nakamura: "Evaluations on contribution of backdrivability and force measurement performance on force sensitivity of actuators", in 2013 IEEE/RSJ International Conference on Intelligent Robots and Systems, pp.4472–4477 (2013)

(18) S. Sakaino and T. Tsuji: "Integration of disturbance observer and feedback modulator for dead zone compensation of hydraulic actuator", in Proceedings of the IEEE 40th Annual Conference of the IEEE Industrial Electronics Society, pp.2786–2791 (2014)

(19) K. Tsuda, T. Sakuma, K. Umeda, S. Sakaino, and T. Tsuji, "Resonance-suppression control for electro-hydrostatic actuator as two-inertia system", *IEEJ Journal of Industry Applications*, Vol.6, No.5, pp.320–327 (2017)

(20) K. Yuki, T. Murakami, and K. Ohnishi: "Vibration control of a 2 mass resonant system by the resonance ratio control", *IEEJ Trans. Industry Applications*, Vol.113, No.10, pp.1162–1169 (1993)

(21) Y. Hori, H. Sawada, and Y. Chun: "Slow resonance ratio control for vibration suppression and disturbance rejection in torsional system", *IEEE Trans. Industrial Electronics*, Vol.46, No.1, pp.162–168 (1999)

(22) Y. Yokokura and K. Ohishi: "Single inertialization of a 2-inertia system based on fine torsional torque and sensor-based resonance ratio controllers", in Proceedings of the 2017 IEEE International Conference on Mechatronics, pp.196–201 (2017)

(23) K. Szabat and T. Orlowska-Kowalska: "Vibration suppression in a two-mass drive system using pi speed controller and additional feedbacks? comparative study", *IEEE Trans. Industrial Electronics*, Vol.54, No.2, pp.1193–1206 (2007)

(24) S.E. Saarakkala and M. Hinkkanen: "State-space speed control of two-mass mechanical systems: Analytical tuning and experimental evaluation", *IEEE Trans. Industry Applications*, Vol.50, No.5, pp.3428–3437 (2014)

(25) R. Oboe and D. Pilastro: "Use of load-side mems accelerometers in servo positioning of two-mass-spring systems", in Proceedings of Proceedings of the 33rd Annual Conference of the IEEE Industrial Electronics, pp.4603–4608 (2015)

(26) S. Yamada, K. Inukai, H. Fujimoto, K. Omata, Y. Takeda, and S. Makinouchi: "Proposal of self resonance cancellation control without using drive-side information", in Proceedings of the 41st Annual Conference of the IEEE Industrial Electronics, pp.783–788 (2015)

(27) K. Sakata, H. Asaumi, K. Hirachi, K. Saiki, and H. Fujimoto: "Self resonance cancellation techniques for a two-mass system and its application to a large-scale stage", *IEEJ Journal of Industry Applications*, Vol.3, No.6, pp.455–462 (2014)

(28) T. Ohgi and Y. Yokokohji: "Control of hydraulic actuator systems using feedback modulator", Journal of Robotics and Mechatronics, Vol.20, No.5, pp.695–708 (2008)

(29) T. Sakuma, K. Tsuda, K. Umeda, S. Sakaino, and T. Tsuji: "Modeling and resonance suppression control for electro-hydrostatic actuator as a two-mass resonant system", *Journal of Advanced Robotics*, pp.1–11 (2017)

(30) S. Sakaino and T. Tsuji: "Resonance suppression of electro-hydrostatic actuator by full state feedback controller using load-side information and relative velocity", in Proceedings of IFAC World Congress 2017 (2017)

(31) M. Aoki, H. Fujimoto, Y. Hori, and T. Takahashi: "Robust resonance suppression control based on self resonance cancellation disturbance observer and application to humanoid robot", in Proceedings of 2013 IEEE International Conference on Mechatronics, pp.623–628 (2013)

(32) S. Sakaino and T. Tsuji: "Development of friction free controller for electro-hydrostatic actuator using feedback modulator and disturbance observer", ROBOMECH Journal, Vol.4, No.1 (2017)

(33) K. Ohnishi, M. Shibata, and T. Murakami: "Motion control for advanced mechatronics", *IEEE/ASME Transactions on Mechatronics*, Vol.1, No.1, pp.56–67 (1996)

(34) K. Umeda, T. Sakuma, K. Tsuda, S. Sakaino, and T. Tsuji: "Reaction force estimation of electro-hydrostatic actuator using reaction force observer", *IEEJ Journal of Industry Applications*, Vol.7, No.3, pp.250–258 (2018)

Sho Sakaino (Senior Member) received the B.E. degree in system design engineering and the M.E. and Ph.D. degrees in integrated design engineering from Keio University, Yokohama, Japan, in 2006, 2008, and 2011, respectively. Since 2011, he has been with Saitama University, Saitama, Japan. Since 2017, he has also been with JST, PRESTO. His research interests include mechatronics, motion control, robotics, and haptics. Dr. Sakaino received the IEEJ Industry Application Societies Distinguished Transactions Paper Award in 2011.

Tomoki Sakuma (Non-member) received the B.E. and M.E. degrees in electrical and electronic system engineering from Saitama University, Saitama, Japan, in 2015 and 2017, respectively. He joined Kawasaki Heavy Industries, Ltd, Hyogo, Japan, in 2017.

Toshiaki Tsuji (Senior Member) received the B.E. degree in system design engineering and the M.E. and Ph.D. degrees in integrated design engineering from Keio University, Yokohama, Japan, in 2001, 2003, and 2006, respectively. He was a Research Associate in the Department of Mechanical Engineering, Tokyo University of Science, from 2006 to 2007. He is currently an Associate Professor in the Department of Electrical and Electronic Systems, Saitama University, Saitama, Japan. His research interests include motion control, haptics and rehabilitation robot. Dr. Tsuji received the FANUC FA and Robot Foundation Original Paper Award in 2007 and 2008.